Supporting Information

Inceoglu et al. 10.1073/pnas.1101073108

SI Materials and Methods

Animals. This study was approved by the University of California, Davis, Animal Care and Use Committee. Male Sprague–Dawley rats weighing 250 to 300 g were obtained from Charles River Laboratories and maintained in University of California, Davis, animal housing facilities with ad libitum water and food on a 12-h/12-h light/dark cycle. A subset of rats was a generous donation from Charles River Laboratories. Data were collected during the same time of day for all groups.

Chemicals. The sEHIs 12-(3-adamantan-1-yl-ureido)-dodecanoic acid (AUDA), TPAU, and TUPS were synthesized as previously reported (1, 2). Rolipram was purchased from Biomol. All other chemicals were obtained from Sigma-Aldrich or Fisher Scientific.

Pain Models. PGE_2-elicited pain was produced by administering PGE_2 (in 10 μL of volume, dissolved in 10% ethanol/90% saline solution) intraplantarly into one hind paw of the rat using a 32-gauge hypodermic needle. Animals were then followed for their nociceptive responses over time as described previously (3). Three different doses of PGE_2 (10, 30, and 100 ng per paw) were administered as detailed in the figure legends.

Behavioral Tests and Treatments. Nociceptive behavioral testing was conducted by observing hindlimb withdrawal responses to thermal and mechanical stimuli, using the Hargreaves, von Frey, and Randall–Selitto tests as described earlier (3, 4). Briefly, animals were acclimated to the testing room and the instrument. Baseline measurements were taken three times at 1-min intervals between measurements. The mean responses of animals were converted to percentages by taking the baseline response of each animal as 100%. For the thermal withdrawal latency test, the baseline values varied between 6 and 10 s. For the von Frey mechanical withdrawal threshold test, the baseline values varied between 70 and 90 g of force. For the Randall–Selitto mechanical withdrawal threshold test, the baseline values varied between 60 and 70 g of force.

For the PGE_2-elicited pain model, the procedure of Khasar et al. was followed with modifications (5). Animals were placed on an elevated steel mesh screen and enclosed in acrylic chambers. Following the baseline von Frey mechanical withdrawal threshold determination, animals were given vehicle, sEHI, celecoxib (20 mg/kg), or dexamethasone (5 mg/kg) s.c. dissolved in PEG400 (Fisher Scientific). One hour after the drug or vehicle administration, PGE_2 was administered into the plantar surface of one hind paw. Animals were then probed with a plastic-tipped force transducer connected to an electronic von Frey analgesiometer (IITC) until a withdrawal response was elicited. The test was conducted by using the maximum holding mode, giving a readout of the highest force in grams applied to the paw. The mean responses of animals were converted to percentages by taking the baseline of each animal as 100%. This baseline value was then subtracted from each data point to obtain a pain scale in which positive values indicate pain and negative values represent analgesia-like lack of pain response. The reduction in pain was calculated by subtracting the mean percent response of the PGE_2 plus vehicle treated animals from the percent response of each PGE_2 plus sEHI treated animal.

For the measurement of acute nociceptive responses, thermal withdrawal latency was measured as described earlier. Additionally, the Randall–Selitto method for quantifying mechanical sensitivity was followed by using an electronic analgesiometer (IITC). Animals were manually restrained and a hind paw was placed between the tapering tip and the flat surface of a hand-held Randall–Selitto apparatus. Force was applied manually until withdrawal was elicited. The test was conducted by using the maximum holding mode, giving a readout of the highest force in grams applied to the paw. Following baseline measurements, compounds (rolipram, TPAU, TUPS, and AUDA) were administered s.c. after dissolving in PEG400. For the PDEi experiments, sEHIs were given 1 h before PDEi. The antagonists fluconazole (40 mg/kg), miconazole (40 mg/kg), or finasteride (10 mg/kg) were dissolved in PEG400 and were given 45 min before PDEi by s.c. injection. Picrotoxin (250 μg/kg) was dissolved in 10% ethanol in saline solution and administered at the same time as sEHI or 45 min before PDEi. For groups treated with PDEi, immediately following the PDEi administration, animals were placed in acrylic chambers on a glass platform maintained at a temperature of 30 ± 1 °C and tested for thermal withdrawal latency measurements. All drug administrations were done s.c. on the backs of the animals away from limbs.

For the measurement of open field activity, animals were placed in an acrylic chamber (40 × 40 × 20 cm length × width × height) divided into 100-cm^2 (10 × 10 cm) sections, and the number of crossings (both hind paws crossing into a neighboring cell) was recorded.

Sampling, Extraction, and Analysis. Blood samples for eicosanoid analysis were collected by using a 24-gauge i.v. catheter (Insyte Autoguard; BD) from the tail vein. Blood was centrifuged and plasma was separated and frozen. All samples were stored at −80 °C until analyses. For the determination of brain inhibitor levels, animals were killed by cardiac puncture while under deep isoflurane anesthesia following inhibitor administration. Animals were perfused with use of cold saline solution to remove traces of blood from brain tissue. The brains were removed following decapitation and frozen on dry ice. The blood and brain levels of TPAU were determined as described previously (4). Briefly, a small (~50 mg) amount of the prefrontal cortex was removed and extracted three times with ethyl acetate containing the internal standard compound 869 [1-adamantan-1-yl-3-(5-butoxy-pentyl)-urea; 250 ng/mL]. The supernatants of three consecutive extractions were pooled and dried before resuspension in 50 μL of methanol. This sample was injected into an HPLC system. The separation was carried out by applying a linear solvent gradient from 10 to 100% acetonitrile in 10 min. The separation module was connected to a Quattro Premier triple-quadrupole mass spectrometer (Waters). The LC electrospray ionization (ESI) MS/MS instrument was operated in positive ESI mode with selected reaction monitoring. The following transitions were monitored: m/z 337.3 > 160 for compound 869 and 346.3 > 169.4 for TPAU. Ionization parameters were same as described previously set to a capillary voltage of 1 kV, cone voltage of 25 V, source temperature of 110 °C, desolvation temperature of 300 °C, and desolvation gas flow of 645 L/h.

Oxylipin analyses were carried out as described by Yang et al. with minor modifications (6). Briefly, an internal standard solution containing deuterated standards was added into the samples. This was followed by extraction of the analytes on a preconditioned solid-phase extraction column (60 mg Oasis-HLB; Waters). The eluted samples were evaporated to dryness and reconstituted in 50 μL of methanol. A 5-μL aliquot of the reconstructed sample solution was directly analyzed by LC–ESI–MS/MS. Separation was carried out on a Agilent 1200 SL LC

system by using an Agilent Zorbax Eclipse Plus C-18 reversed-phase column (2.1 × 150 mm, 1.8 μM particle size) with a gradient of 0.1% acetic acid as solvent A and 80/15/0.1 acetonitrile/methanol/acetic acid as solvent B. The oxylipins were separated within 21 min by using a similar gradient as described by Yang et al. (6). The column was reconditioned for 3.4 min at 35% solvent B before the next sample was introduced.

The detection was carried out using a 4000 QTRAP instrument (Applied Biosystems) operating in negative ion mode as previously described (6) by monitoring the following selected reaction monitoring transitions: 9(10)-EpOME (*m/z* 295/171), 9,10-DiHOME (*m/z* 313/201), 12(13)-EpOME (*m/z* 295/195), 12,13-DiHOME (*m/z* 313/183), 8(9)-EpETrE (*m/z* 319/167), 8,9-DiHETrE (*m/z* 337/127), 11(12)-EpETrE (*m/z* 319/167), 11,12-DiHETrE (*m/z* 337/167), 14(15)-EpETrE (*m/z* 319/219), 14,15-DiHETrE (*m/z* 337/207), 8(9)-EpETE (*m/z* 317/127), 8,9-DiHETE (*m/z* 335/127), 11(12)-EpETE (*m/z* 317/167), 11,12-DiHETE (*m/z* 335/167), 14(15)-EpETE (*m/z* 317/207), 14,15-DiHETE (*m/z* 335/207), 17(18)-EpETE (*m/z* 317/215), 17,18-DiHETE (*m/z* 335/247), 10(11)-EpDPE (*m/z* 343/153), 10,11-DiHDPE (*m/z* 361/153), 13(14)-EpDPE (*m/z* 343/193), 13,14-DiHDPE (*m/z* 361/193), 16(17)-EpDPE (*m/z* 343/233), 16,17-DiHDPE (*m/z* 361/233), 19(20)-EpDPE (*m/z* 343/241), and 19,20-DiHDPE (*m/z* 361/273).

Enzyme Assays and Synthesis of Inhibitors. Inhibitory potencies of the sEHIs were determined by using a modified procedure as described previously (4, 7). Recombinant enzymes cloned from mouse, rat, and human were expressed by a baculovirus expression system followed by purification through an affinity chromatography step (7). Pierce BCA assay was used to quantify protein amounts. The concentration that leads to the inhibition of half of the enzyme activity by an inhibitor was assigned as the IC_{50} for that compound. Potency on recombinant sEH from the mouse, rat, and human were determined by using a fluorescent substrate, cyano(2-methoxynaphthalen-6-yl)methyl trans(3-phenyloxyran-2-yl) methyl carbonate (8). Rolipram was tested for inhibitory activity by using recombinant human and rat enzymes by incorporating 10 and 100 μM of rolipram into the sEH assay. No inhibition was observed by rolipram. Each IC_{50} experiment included at least five different concentrations of inhibitor determined in triplicate. For rolipram, only two concentrations were used. Inhibitors of sEH were synthesized, purified, and characterized in our laboratory as described previously (1, 9).

Statistical Analyses. Data were analyzed by ANOVA followed by Dunnett two-sided *t* test for between-group comparisons with the SPSS analysis package (SPSS). Results are depicted as mean ± SEM. Regression equations were used for the calculation of IC_{50} values.

SI Discussion

Selection of sEH and PDE Inhibitors. The structurally different inhibitors of sEH used in this study were selected based on several criteria. By using multiple sEHI with different structures, potencies, and pharmacokinetic properties, we tested the hypothesis that inhibition of sEH, rather than compound-specific effects, are responsible for the observed biological effects. The sEHI TPAU, compared with other sEHIs, is moderately potent (Table S3). However, TPAU has a long half-life and excellent demonstrated bioactivity on inflammatory pain (4), which may be attributed to its ability to penetrate into the brain (Fig S2). TUPS, on the contrary, is at least eight times more potent than TPAU, has a long half-life, and penetrates into the brain. AUDA, an early prototype sEHI, is highly potent but has a much shorter half-life than the other two sEHIs. Thus, doses of sEHIs selected in this study (TPAU, 10 mg/kg; TUPS, 3 mg/kg; and AUDA, 40 mg/kg) reflect their potency and in vivo stability. Table S3 displays the structures and in vitro potencies of sEHIs used in this study. Regardless of the differences in these three compounds we observed the same pattern of biological activity with all three sEHI.

The inhibitors of PDE were selected based on their ability to inhibit different PDE isozymes. We investigated the effects of a nonselective PDEi, pentoxifylline, a selective PDE3i, cilostamide, two selective PDE4is, rolipram and YM976, and a selective PDE5i, TO-156. For the quantification of oxylipins, the nonselective PDEi was used at 10 mg/kg because we expected to observe lower efficacy for this compound. All other PDEis were tested at a dose of 1 mg/kg.

Pharmacological Characterization of Rolipram and sEHI/Rolipram. Few non-ion channel, nonneurotransmitter molecules are known to influence sensory function (10). Therefore, it was surprising to find that inhibition of sEH can have a profound effect on acute nociceptive thresholds when given together with a PDEi (Fig. 2). To understand the mechanism of this observation, we investigated the pharmacological profile of the interaction between elevated cAMP and EFAs. To this end, we asked if the effects of the sEHI/rolipram treatment are distinguishable from rolipram alone by using a group of antagonists selected based on our previous work with sEHI (4). First, we tested if a COX-2–selective inhibitor, celecoxib, interacted with cAMP elevated by PDEi. Celecoxib, at a single 20-mg/kg dose, was administered 30 min before increasing doses of rolipram and thermal withdrawal latency was monitored over 4 h (Fig. S6*A*). One hour after rolipram administration, celecoxib did not change rolipram's ability to elevate acute pain thresholds, indicating that there is minimal interaction between the cyclooxygenase and cAMP pathways. This finding also supports the hypothesis that sEHIs are distinct pharmacological agents that act through mechanisms independent from their suppression of the cyclooxygenase expression (4). Indeed, reducing pain produced by PGE_2 also strongly demonstrates that sEHI are a new class of pain-reducing agents (Fig. 1*A*).

Next, based on our previous observations that blocking of the steroid synthesis pathway with aminoglutethimide and finasteride were antagonistic to sEHI-mediated antihyperalgesia, we hypothesized that neurosteroids are involved in the mode of action of sEHI (4). The molecular targets of neurosteroids are believed to be the GABA complex channels (11, 12). Accordingly, we used a $GABA_A$ antagonist, picrotoxin, to test if sEHIs augment GABA-mediated signaling. A dose of picrotoxin that was inactive by itself was selected to antagonize rolipram and sEHI/rolipram. This dose of picrotoxin (0.25 mg/kg s.c.) was not only ineffective on its own in changing pain-related behavior, but was also possibly too low to cause analgesia by way of inhibiting spinal nociceptive neurons that regulate the descending antinociceptive system (13). Here, another structurally different sEHI, AUDA, was used. AUDA, similar to TPAU, synergistically reduced pain-related behavior when coadministered with rolipram, elevating thermal withdrawal latency and mechanical withdrawal thresholds, two important measures of pain status (Fig. S5 *B* and *C*). AUDA was ineffective on its own in changing pain-related behavior in rats (4). Picrotoxin strongly antagonized the effects of AUDA/rolipram but partially antagonized rolipram (Fig. S5*B*). Furthermore, the effects of picrotoxin were different in regard to antagonizing thermal versus mechanical withdrawal responses (Fig. S5*C*). This selective antagonism argues that picrotoxin did not act as a stimulant that restored the PDEi-suppressed general nervous system activity. Therefore, we propose the involvement of $GABA_A$ receptors in sEHI-mediated antinociception. In addition, a neurosteroid synthesis inhibitor and a formerly demonstrated sEHI antagonist in an inflammatory pain model, finasteride, acted as a competitive antagonist of rolipram (Fig. S5*D*).

To further understand the contribution of epoxygenated fatty acids to the effect of rolipram, we blocked the de novo synthesis of

EFAs by using a CNS-permeable cytochrome P450 epoxygenase inhibitor, fluconazole (Fig. S5*E*). Antagonism produced by fluconazole was noncompetitive and nonsurmountable. This suggests that only a portion of the reduction in pain related behavior produced by rolipram is dependent on EFAs. The CNS-impermeable epoxygenase inhibitor miconazole completely lacked antagonistic effect, strongly arguing that CNS effects of rolipram prevail over peripheral effects. Furthermore, the sEHI treatment in non-inflamed animals led to elevated epoxide/diol ratio but, unlike rolipram, not to increases in nociceptive thresholds or motor depression (Fig. 1). Additionally, coadministration of sEHI/rolipram produced an additive increase in the plasma epoxy/diol fatty acid ratio while synergistically elevating nociceptive thresholds. Overall, these observations strongly argue that rolipram acts distinctly from sEHI plus rolipram. However, a considerable portion of rolipram's antinociceptive effect seems to be dependent on EFAs.

Quantitative Metabolomic Analysis of Substrates and Products of the sEH. The plasma levels of epoxygenated fatty acids are globally affected when the sEH is inhibited. We analyzed metabolites from linoleic acid, ARA, docosahexaenoic acid, and eicosapentaenoic acid, quantifying the EFAs and their corresponding degradation products by sEH the dihydroxy-FAs to assess the effects of inhibiting sEH and PDE4. These analyses allowed us to correlate inhibition of enzymes with plasma biomarkers and the observed biological activity. Inhibition of sEH and PDE4 demonstrated highly significant changes in EFA levels (Fig. 3 *A* and *B*). However, inhibition of sEH and PDE4 were qualitatively and quantitatively distinct in the manner that they affected EFAs (Fig. S4). In particular, the inhibition of sEH elevated EFAs as well as significantly decreased the dihydroxy-FAs (Table S1). On the contrary, the inhibition of PDE4, in general, elevated the EFAs but also the dihydroxy-FAs, also supporting the finding that PDE4 inhibitors do not inhibit sEH. The PDE4 inhibitor mediated increase in the dihydroxy-FAs is not unexpected because, in the absence of an sEHI, the EFAs are rapidly degraded to the dihydroxy-FAs. In support of this argument the coadministration of sEHI plus PDE4i led to increase in EFAs and decrease in dihydroxy-FA levels (Fig. 3 and Table S1). In investigating a series of PDE inhibitors including a general inhibitor (pentoxifylline), a PDE3-selective inhibitor (cilostamide), an additional PDE4-selective inhibitor (YM976), and a PDE5-selective inhibitor (TO-156), we demonstrate that many isozyme-selective PDE inhibitors elevate the levels of EFAs (Table S2). Because all these inhibitors are selective and not specific, they inhibit multiple isozymes at varying potencies. Therefore, it is not possible to conclude if the PDE5-selective inhibitor elevated EFAs because of inhibition of PDE4 or PDE5. Overall, most PDE inhibitors seem to affect EFAs, and some selective PDEi are as effective as potent sEHI in this regard. These data demonstrate that part of the bioactivity of PDEi on various physiological processes is by way of modulating the levels of EFAs and dihydroxy-FAs.

1. Jones PD, Tsai H-J, Do ZN, Morisseau C, Hammock BD (2006) Synthesis and SAR of conformationally restricted inhibitors of soluble epoxide hydrolase. *Bioorg Med Chem Lett* 16:5212–5216.
2. Morisseau C, et al. (2002) Structural refinement of inhibitors of urea-based soluble epoxide hydrolases. *Biochem Pharmacol* 63:1599–1608.
3. Inceoglu B, et al. (2006) Inhibition of soluble epoxide hydrolase reduces LPS-induced thermal hyperalgesia and mechanical allodynia in a rat model of inflammatory pain. *Life Sci* 79:2311–2319.
4. Inceoglu B, et al. (2008) Soluble epoxide hydrolase and epoxyeicosatrienoic acids modulate two distinct analgesic pathways. *Proc Natl Acad Sci USA* 105:18901–18906.
5. Khasar SG, Ho T, Green PG, Levine JD (1994) Comparison of prostaglandin E1- and prostaglandin E2-induced hyperalgesia in the rat. *Neuroscience* 62:345–350.
6. Yang J, Schmelzer K, Georgi K, Hammock BD (2009) Quantitative profiling method for oxylipin metabolome by liquid chromatography electrospray ionization tandem mass spectrometry. *Anal Chem* 81:8085–8093.
7. Wixtrom RN, Hammock BD (1988) Continuous spectrophotometric assays for cytosolic epoxide hydrolase. *Anal Biochem* 174:291–299.
8. Jones PD, et al. (2005) Fluorescent substrates for soluble epoxide hydrolase and application to inhibition studies. *Anal Biochem* 343:66–75.
9. Morisseau C, Hammock BD (2007) Measurements of soluble epoxide hydrolase (sEH) activity. *Techniques for Analysis of Chemical Biotransormation. Current Protocols in Toxicology*, eds Bus JS, Costa LG, Hodgson E, Lawrence DA, Reed DJ (Wiley, New York), pp 4.23.1–4.23.18.
10. Willis WD, Jr., Coggeshall RE (2004) *Sensory Mechanisms of the Spinal Cord* (Kluwer/Plenum, New York).
11. Morrow AL (2007) Recent developments in the significance and therapeutic relevance of neuroactive steroids—Introduction to the special issue. *Pharmacol Ther* 116:1–6.
12. Belelli D, Lambert JJ (2005) Neurosteroids: Endogenous regulators of the GABA(A) receptor. *Nature Reviews Neuroscience* 6:565–575.
13. Koyama N, Hanai F, Yokota T (1998) Does intravenous administration of GABAA receptor antagonists induce both descending antinociception and touch-evoked allodynia? *Pain* 76:327–336.

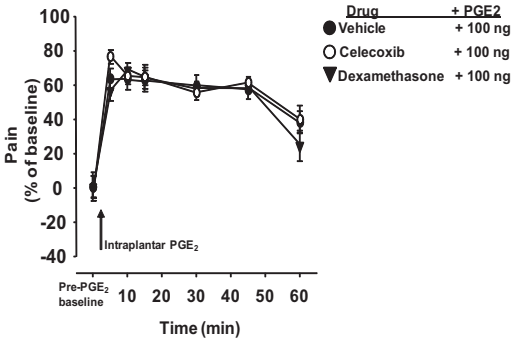

Fig. S1. A selective COX-2 inhibitor and a steroidal anti-inflammatory drug are ineffective in reducing pain produced by the COX product PGE_2. Pain was induced by a single intraplantar injection of PGE_2 (100 ng per paw in 10 μL solution containing 10% DMSO) into one hind paw of rat and quantified by von Frey assay. Drugs were administered following baseline measurements, 1 h before PGE_2 administration. COX inhibitors and steroidal anti-inflammatory drugs act by reducing COX enzyme activity and expression, respectively. Therefore, pain produced by a product downstream to cyclooxygenases is expectedly impervious to reversal by celecoxib (20 mg/kg s.c.) or dexamethasone (5 mg/kg s.c.). All data in figures are presented as mean ± SEM. The *y* axis is the difference in percentage change in mechanical withdrawal threshold compared with before PGE_2 administration (n = 6 in all groups). On some graphs, the SEM bars are not visible because they are smaller than the symbol representing the data point. In contrast, TUPS and TPAU are effective in reducing pain in this system and work downstream from PGE_2 (Fig. 1).

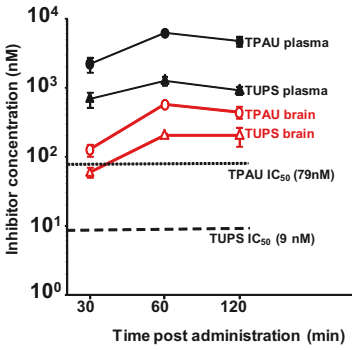

Fig. S2. Plasma and brain tissue levels of sEHI. Both compounds were dissolved in PEG400 and administered s.c. A dose of 10 mg/kg of TPAU and a dose of 3 mg/kg TUPS were administered (n = 4 per group).

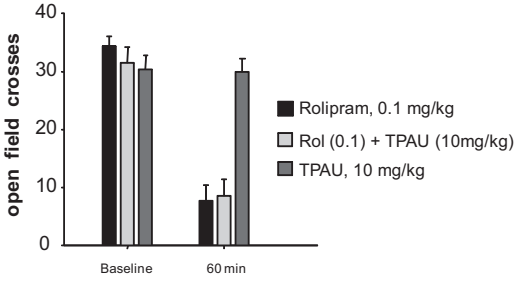

Fig. S3. Motor depressant effect of rolipram. Rolipram, as expected, led to a significant and dose-dependent decrease in voluntary movement in an open-field chamber even 1 h following administration. In contrast, TPAU treatment was indistinguishable from baseline activity. The combination of TPAU plus rolipram led to a similar degree of motor depression, but this depression as rolipram alone, unlike the synergistic analgesia produced, was not potentiated by the combination.

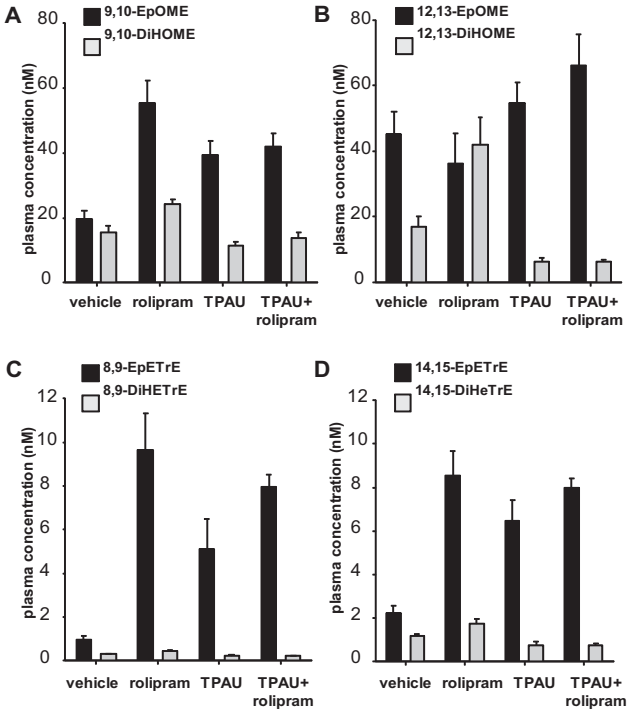

Fig. S4. Qualitative and quantitative differences between sEHI- and PDEi-mediated changes in EFAs and dihydroxy-FAs. Plasma levels of four groups of EFAs and their corresponding hydrolysis products as indicated on the panels are demonstrated in (*A*) 9,10- EpOME and 9,10-DiHOME and (*B*) 12,13-EpOME and 12,13-DiHOME. In particular, rolipram administration mediated no increase in leukotoxin (12,13-EpOME) levels but a significant elevation of the threefold more toxic leukotoxin diol (12,13-DiHOME) levels. Most other EFAs were elevated by rolipram, indicating that PDEis selectively modulate the levels of these bioactive lipid metabolites. The inhibitor of sEH elevated all EFAs quantified. These data are consistent with changes in EETs as demonstrated (*C* and *D*) (Fig. 4). Coadministration of rolipram and sEHI elevated the levels of EFAs. The undesirable increase in leukotoxin diol was ameliorated when rolipram and TPAU were coadministered.

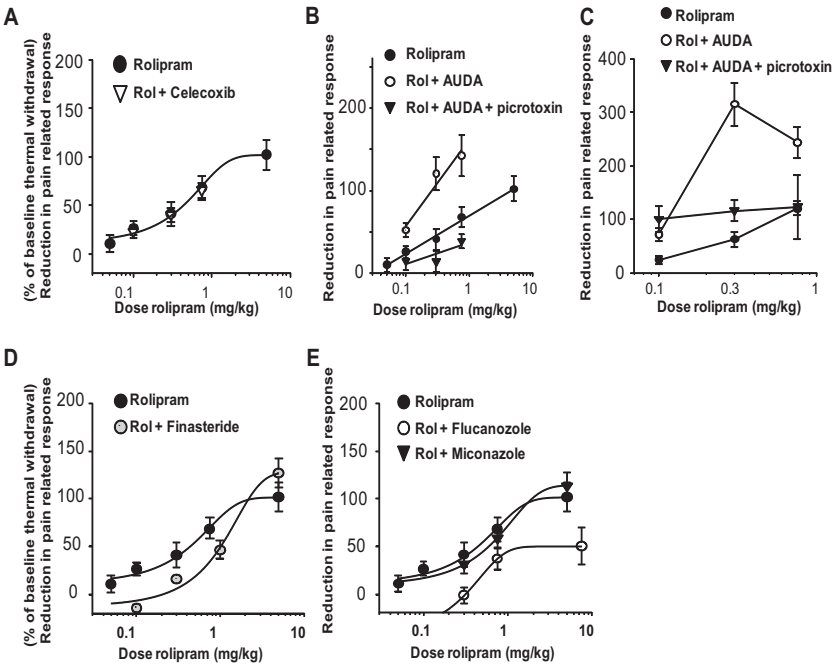

Fig. S5. Rolipram- and sEHI/rolipram-mediated changes in nociceptive thresholds are pharmacologically distinct. (*A*) A selective COX-2 inhibitor, celecoxib, did not demonstrate any interaction with the PDE4 inhibitor rolipram, indicating that elevated cAMP is not required for COX inhibitors. (*B*) The GABA antagonist picrotoxin effectively antagonized the increases in thermal withdrawal latency produced by rolipram/AUDA but partially blocked rolipram. (*C*) The GABA antagonist picrotoxin effectively antagonized the increases in mechanical withdrawal threshold produced by rolipram/AUDA but not that of rolipram itself. Here, nociceptive thresholds are measured by Randall–Selitto mechanical sensitivity assay. (*D*) Line graph of competitive antagonism of the PDE4i rolipram produced antinociception by finasteride, a neurosteroid synthesis inhibitor. Here nociceptive thresholds are measured by Hargreaves thermal withdrawal latency assay. (*E*) Noncompetitive antagonism of rolipram by fluconazole (40 mg/kg), an inhibitor of epoxygenases in the CNS, and lack of antagonism by micanozole (40 mg/kg), a CNS-impermeable epoxygenase inhibitor. Nociceptive thresholds are measured by Hargreaves thermal withdrawal latency assay (n = 6 per group in all panels).

Table S1. Quantitative analysis (mean ± SEM) of endogenous oxylipin sEH substrates and products in rat plasma following sEHI (TPAU) and rolipram administration

Parent fatty acid/metabolite oxylipin	Vehicle, nM	Rolipram, nM	TPAU, nM	TPAU/rolipram, nM
Linoleate C18:2				
9(10)-EpOME	19.6 ± 2.4	55.2 ± 7.1	39.2 ± 4.4	42.0 ± 3.8
9,10-DiHOME	15.5 ± 2.1	24.3 ± 1.4	11.5 ± 1.0	13.7 ± 1.6
Ratio	1.2	2.2	3.4	3.0
12(13)-EpOME	45.0 ± 6.9	36.3 ± 9.0	54.7 ± 6.3	66.0 ± 9.4
12,13-DiHOME	17.0 ± 3.1	42.0 ± 8.2	6.3 ± 1.0	6.1 ± 0.5
Ratio	2.6	0.86	8.6	10.7
Arachidonate C20:4				
8(9)-EpETrE	1.0 ± 0.1	9.6 ± 1.6	5.1 ± 1.3	7.9 ± 0.5
8,9-DiHETrE	0.3 ± 0.03	0.45 ± 0.04	0.22 ± 0.03	0.23 ± 0.01
Ratio	3.3	21.2	23.3	34.4
11(12)-EpETrE	2.4 ± 0.4	13.1 ± 2.2	10.4 ± 2.0	11.8 ± 0.8
11,12-DiHETrE	1.4 ± 0.1	1.6 ± 0.1	1.2 ± 0.2	1.1 ± 0.1
Ratio	1.6	7.8	8.3	10.0
14(15)-EpETrE	2.2 ± 0.3	8.5 ± 1.1	6.4 ± 0.9	7.9 ± 0.4
14,15-DiHETrE	1.1 ± 0.1	1.7 ± 0.1	0.78 ± 0.1	0.77 ± 0.09
Ratio	1.9	4.8	8.3	10.3
Eicosapentanoate C20:5				
8(9)-EpETE	0.13 ± 0.05	1.2 ± 0.2	0.8 ± 0.2	1.1 ± 0.1
8,9-DiHETE	0.12 ± 0.04	0.07 ± 0.01	0.06 ± 0.01	0.04 ± 0.004
Ratio	1.0	18.1	14.0	28.2
11(12)-EpETE	0.05 ± 0.02	0.93 ± 0.18	0.51 ± 0.09	0.78 ± 0.11
11,12-DiHETE	0.12 ± 0.04	0.20 ± 0.02	0.13 ± 0.01	0.13 ± 0.01
Ratio	0.14	4.7	4.0	6.1
14(15)-EpETE	0.48 ± 0.11	0.84 ± 0.14	0.54 ± 0.06	0.76 ± 0.11
14,15-DiHETE	0.70 ± 0.07	0.28 ± 0.04	0.15 ± 0.02	0.12 ± 0.02
Ratio	0.68	2.9	3.6	6.3
17(18)-EpETE	1.7 ± 0.3	1.7 ± 0.2	1.2 ± 0.1	1.3 ± 0.1
17,18-DiHETE	2.0 ± 0.2	0.77 ± 0.12	0.40 ± 0.05	0.34 ± 0.03
Ratio	0.86	2.3	3.2	3.9
Docosahexanoate C22:6				
10(11)-EpDPE	2.2 ± 0.4	7.5 ± 1.3	5.6 ± 1.0	6.7 ± 0.6
10,11-DiHDPE	0.50 ± 0.04	0.33 ± 0.03	0.23 ± 0.03	0.20 ± 0.02
Ratio	4.5	22.8	24.1	34.5
13(14)-EpDPE	1.2 ± 0.2	3.8 ± 0.6	2.9 ± 0.5	3.4 ± 0.3
13,14-DiHDPE	0.64 ± 0.07	0.37 ± 0.03	0.36 ± 0.06	0.25 ± 0.02
Ratio	1.9	10.5	8.1	13.6
16(17)-EpDPE	1.7 ± 0.1	3.9 ± 0.63	3.1 ± 0.5	3.5 ± 0.3
16,17-DiHDPE	1.5 ± 0.3	0.72 ± 0.08	0.50 ± 0.10	0.39 ± 0.03
Ratio	1.1	5.4	6.1	8.9
19(20)-EpDPE	8.0 ± 0.7	7.4 ± 0.8	5.9 ± 0.8	5.6 ± 0.3
19,20-DiHDPE	5.3 ± 1.2	2.1 ± 0.1	1.6 ± 0.2	1.2 ± 0.06
Ratio	1.5	3.5	3.6	4.4
Sum				
EFA	86.0	150.4	136.7	159.2
Dihydroxy-fatty acid	46.5	75.1	23.6	24.8
Ratio	1.85	2.0	5.8	6.4

The oxylipins were quantified according to the methods and references. Drugs were administered s.c., and blood was taken 60 min following TPAU (10 mg/kg, $n = 6$), rolipram (1 mg/kg, $n = 12$), and TPAU/rolipram (10 and 1 mg/kg, respectively, $n = 6$). Below, oxylipins are grouped based on their parent molecules, linoleic acid, ARA, docosahexaenoic acid, and eicosapentaenoic acid (first column). The mean and SE (SEM) of the determined concentration (in nM) is presented. Ratio of epoxy/dihydroxy eicosanoids for each epoxide/diol pair is also shown. The SEM for ratios was omitted for clarity. The graphs presented in Fig. 3 include sum of ARA, docosahexaenoic acid, and eicosapentaenoic acid metabolites listed here. Fig. S2 shows plasma levels of TPAU at the time of sampling.

Table S2. Quantitative analysis of endogenous oxylipin sEH substrates and products in rat plasma following PDE inhibitor administration

Parent fatty acid/metabolite oxylipin	Pentoxyphilline, nM (n = 3)	Cilostamide, nM (n = 4)	TO-156, nM (n = 3)	YM976, nM (n = 6)
Linoleate C18:2				
9(10)-EpOME	32.4 ± 19.8	34.2 ± 7.4	60.0 ± 13.0	147.0 ± 82.3
9,10-DiHOME	29.5 ± 8.1	38.3 ± 4.5	34.2 ± 4.5	37.0 ± 8.8
Ratio	1.1	0.89	1.7	3.9
12(13)-EpOME	51.8 ± 22.8	63.3 ± 10.4	87.0 ± 22.3	159.3 ± 62.7
12,13-DiHOME	37.9 ± 11.7	53.5 ± 6.4	50.8 ± 3.8	57.3 ± 17.8
Ratio	1.3	1.1	1.7	2.7
Arachidonate C20:4				
8(9)-EpETrE	3.1 ± 1.4	3.6 ± 1.3	6.4 ± 0.3	13.5 ± 7.7
8,9-DiHETrE	0.47 ± 0.07	0.49 ± 0.03	0.54 ± 0.01	0.58 ± 0.11
Ratio	6.6	7.4	11.9	23.4
11(12)-EpETrE	4.4 ± 2.1	5.4 ± 2.10	10.6 ± 0.5	22.8 ± 12.9
11,12-DiHETrE	1.6 ± 0.3	1.9 ± 0.13	1.7 ± 0.1	1.5 ± 0.2
Ratio	2.7	2.8	6.0	14.7
14(15)-EpETrE	7.7 ± 3.0	8.6 ± 2.49	14.7 ± 0.7	26.5 ± 12.6
14,15-DiHETrE	1.8 ± 0.2	1.7 ± 0.04	1.7 ± 0.03	1.8 ± 0.2
Ratio	4.2	5.0	8.5	14.4
Eicosapentanoate C20:5				
8(9)-EpETE	0.74 ± 0.3	0.72 ± 0.29	1.2 ± 0.2	2.7 ± 1.4
8,9-DiHETE	0.27 ± 0.1	0.20 ± 0.04	0.3 ± 0.04	0.29 ± 0.03
Ratio	2.8	3.5	4.1	9.6
11(12)-EpETE	0.45 ± 0.21	0.50 ± 0.19	0.80 ± 0.07	2.2 ± 1.2
11,12-DiHETE	0.43 ± 0.11	0.35 ± 0.04	0.45 ± 0.05	0.48 ± 0.08
Ratio	1.0	1.4	1.7	4.6
14(15)-EpETE	0.49 ± 0.21	0.55 ± 0.17	0.69 ± 0.04	1.9 ± 0.9
14,15-DiHETE	1.2 ± 0.32	0.82 ± 0.13	1.0 ± 0.12	1.1 ± 0.1
Ratio	0.39	0.6	0.66	1.6
17(18)-EpETE	2.6 ± 0.6	2.3 ± 0.25	3.0 ± 0.4	4.4 ± 1.1
17,18-DiHETE	3.0 ± 0.6	1.7 ± 0.14	2.8 ± 0.4	2.9 ± 0.2
Ratio	0.86	1.3	1.1	1.5
Docosahexanoate C22:6				
10(11)-EpDPE	4.0 ± 2.0	3.4 ± 1.40	7.8 ± 0.8	20.1 ± 11.4
10,11-DiHDPE	0.66 ± 0.18	0.54 ± 0.05	0.71 ± 0.1	0.82 ± 0.13
Ratio	6.1	6.4	8.5	24.5
13(14)-EpDPE	2.2 ± 1.0	1.8 ± 0.74	4.2 ± 0.53	10.2 ± 5.6
13,14-DiHDPE	0.73 ± 0.19	0.64 ± 0.05	0.79 ± 0.08	0.81 ± 0.09
Ratio	3.0	2.9	11.1	12.6
16(17)-EpDPE	2.9 ± 1.3	2.4 ± 0.80	5.0 ± 0.70	10.4 ± 5.2
16,17-DiHDPE	2.2 ± 0.51	1.6 ± 0.19	2.2 ± 0.35	2.2 ± 0.20
Ratio	1.2	1.5	5.3	4.6
19(20)-EpDPE	8.9 ± 2.3	6.6 ± 0.96	12.0 ± 2.0	18.1 ± 6.0
19,20-DiHDPE	5.5 ± 0.9	4.0 ± 0.21	6.0 ± 1.1	6.2 ± 0.5
Ratio	1.6	1.6	2.3	2.9
Sum				
EFA	122.0	133.7	213.7	439.6
Dihydroxy-fatty acid	85.5	105.9	103.4	113.3
Ratio	1.4	1.2	2.0	3.8

The oxylipins were quantified according to the methods outlined in the text. Drugs were administered s.c., and blood was taken 45 min following administration. Compounds were dissolved in PEG400 and administered at a dose of 1 mg/kg except for pentoxyphilline, which was 10 mg/kg. Below, oxylipins were grouped based on their parent molecules, linoleic acid, ARA, docosahexaenoic acid, and eicosapentaenoic acid (first column). The mean and SE (SEM) of the determined concentration in nM is presented. Ratio of epoxy/dihydroxy eicosanoids for each epoxide/diol pair is shown in red color. The SEM for ratios was omitted for clarity. The graphs presented in Fig. 3 includes sum of ARA, docosahexaenoic acid, and eicosapentaenoic acid metabolites. Table S1 shows for vehicle administered control group.

Table S3. Structures and potencies of inhibitors used on recombinant sEH

Name	Structure	IC_{50}, nM*		
		Human	Mouse	Rat
AUDA		3	10	11
TPAU	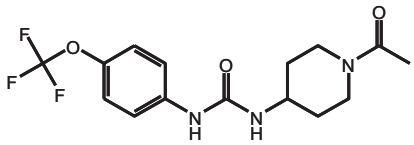	12	97	79
TUPS	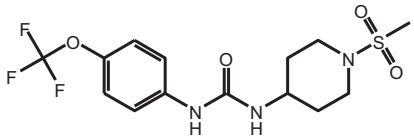	3	5	9
Rolipram	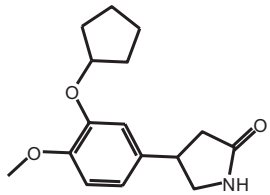	>10,000	>10,000	>10,000

Potency determined using recombinant enzymes purified to homogeneity by affinity chromatography and the fluorescent substrate cyano (2-methoxynaphthalen-6-yl)methyl *trans*-(3-phenyl-oxyran-2-yl) methyl carbonate. Nanomolar concentrations of homogenous enzyme in the assay solution were used to determine IC_{50} values.

*IC_{50} values are relative expression of the potency of the inhibitors. The value for an inhibitor with a particular enzyme will vary as a function of the substrate used and the assay conditions. As an example, when we tested the IC_{50} values for AUDA, TPAU, and TUPS using a synthetic radiolabeled substrate, *t*-DPPO (racemic [^{3}H]-*trans*-1,3-diphenylpropene oxide) and recombinant human sEH, we found that the potency of AUDA, TPAU, and TUPS was 10, 160, and 120 nM, respectively. When a natural substrate, 14(15)-EpETrE, was used in a LC-MS/MS–based inhibition assay, we obtained IC_{50} values on recombinant human sEH for AUDA and TUPS that were 7.3 $\pm$ 3 and 5.5 $\pm$ 2 nM, respectively. Moreover, changing the assay conditions, such as enzyme or substrate concentration, even within each one of the different assays, may result in different IC_{50} values. Thus, a range of values are obtained under different conditions.